33rd Annual International Conference of the IEEE EMBS
Boston, Massachusetts USA, August 30 - September 3, 2011

Reconfigurable MRI-Guided Robotic Surgical Manipulator: Prostate Brachytherapy and Neurosurgery Applications

Hao Su†, Iulian I. Iordachita†, Xiaoan Yan, Gregory A. Cole and Gregory S. Fischer

Abstract— **This paper describes a modular design approach for robotic surgical manipulator under magnetic resonance imaging (MRI) guidance. The proposed manipulator provides 2 degree of freedom (DOF) Cartesian motion and 2-DOF pitch and yaw motion. Primarily built up with dielectric materials, it utilizes parallel mechanism and is compact in size to fit into the limited space of close-bore MRI scanner. It is ideal for needle based surgical procedures which usually require positioning and orientation control for accurate imaging plane alignment. Specifically, this mechanism is easily reconfigurable to over constrained manipulator structure which provides 2-DOF Cartesian motion by simple structure modification. This modular manipulator integrated with different end-effector modules is investigated for prostate brachytherapy and neurosurgery applications as preliminary evaluation.**

I. INTRODUCTION

MAGNETIC resonance imaging can provide high resolution multi-parametric imaging, large soft tissue contrast, and interactive image updates making it an ideal guidance modality for a number of surgical interventions. Nevertheless, there are many challenges to successful deployment of robotic system in MRI environment. Two major facets contribute to the complexity engendered in mechanical design, actuation and sensing. First, the magnetic field gradients and radio frequency pulses of MRI might induce electrical currents in conductive materials, which may cause considerable heating and distortion of the field homogeneity. Ferromagnetic and highly paramagnetic materials, which are cornerstone construction materials of generic robotic systems, are prohibited inside and around the scanner. Second, traditional actuators that rely upon electromagnetic principles are also prohibited due to the lack of bidirectional compatibility: the electromagnetic field and electrical signals of the motors would deteriorate MR image quality and the MRI scanner could affect motor operation. To address these issues, a number of technical approaches have been proposed.

A. Mechanisms for MRI-guided Surgical Interventions

While methods to ameliorate the first restriction is conceptually simple and robotic systems can be constructed with dielectric materials (primarily plastics and ceramics). However, the mechanical properties of these materials are inferior to their metallic counterparts, which makes mechanism imperative for successful robotic structure design. Moreover, it requires deliberate design consideration that minimizes the transverse space of the closed-bore. To comply with this restriction, a number of mechanisms have been investigated: (i) remote center of motion (RCM) mechanism using arch structure [1] and parallelogram, (ii) articulated serial linkage mechanism [2] and a more generic modular approach [3], (iii) a 5-DOF parallel manipulator [4], (iv) compliant mechanism, including bending mechanism of micro grasping forceps for neurosurgery [5] and leverage and parallelepiped mechanism for micro surgery [6], (v) continuum type robot utilizing steerable needles [7] and (vi) a wire-driven needle angulation mechanism [8].

H. Su, X. Yan, G.A. Cole and G.S. Fischer are with the Automation and Interventional Medicine (AIM) Laboratory in the Department of Mechanical Engineering. Worcester Polytechnic Institute, Worcester, MA, USA haosu@wpi.edu, gfischer@wpi.edu

I. Iordachita is with the Laboratory for Computational Science and Robotics, Johns Hopkins University, Baltimore, MD, USA iordachita@jhu.edu

†Shared first authorship.

B. Actuation Methods for MRI-guided Surgical Robots

MRI-guided robots have been developed for prostate interventions [9]–[12], neurosurgery [13], cardiac surgeries [14] and breast biopsy [15]. Four actuation principles have been utilized in these applications, namely remote actuation, hydraulic, pneumatic and ultrasonic/piezoelectric actuators. Remote actuation suffers from bulky structure, low bandwidth and lower resolution and is not preferable for robotic applications. Hydraulic and pneumatic actuation can completely avoid electrical and magnetic noise and the latter has been deployed in a number of systems. Piezoelectric motors using commercially available motor controllers negatively impacted image quality. Generally, pneumatic and piezoelectric actuations are the primary armamentarium for robotic applications in MRI.

C. Contribution and Organization

In our previous studies, we have developed three robotic modules to aid the needle placement, namely a Cartesian positioning module, needle driver module, a RCM stereotactic frame module [7], [13]. As for the Cartesian positioning module, it is advantageous because of the decoupled kinematics and scissor mechanism to increase system rigidity. However, the proposed system in this paper includes four merits: (1) orientation control of the pitch angle to facilitate the avoidance of pubic arch interference (PAI); (2) isotropic stiffness enhancement in the lateral and axial directions; (3) the new robot has a pyramid-like shape that is compact in size and in particular utilizes the space "under the leg" for prostate intervention; and (4) the new design circumvents the needle driver axial rotation issue in the previous development [16].

Although developed as a general reconfigurable module, we use two case studies (prostate brachytherapy and neurosurgery) as shown in Fig. 1 to highlight benefits of such parallel mechanism based modular design. This paper is organized as follows: Section II describes the system concept and design requirements for both procedures. Section

III presents mechanism design, kinematics and workspace analysis. Preliminary evaluation of the system and integration with other surgical end-effectors is presented in Section IV to illustrate the manipulator modularity. Finally, a discussion of the system is presented in Section V.

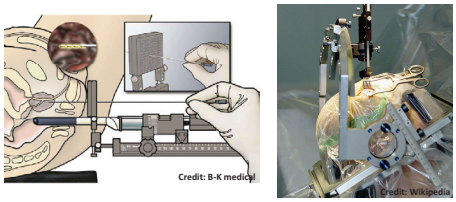

Fig. 1. Two targeted surgical applications of this modular design approach: MRI-guided prostate biopsy and brachytherapy (left) and stereotactic neurosurgery for deep brain stimulation (right).

II. System Concept and Design Requirements

The guiding vision of this mechanism design inside MRI has two major considerations: First, the building materials are primarily plastics thus structural rigidity is imperative for robot design. Second, since the target application for high-field MRI whose close-bore has a cylindrical shape with diameter around $70cm$, the mechanism needs to minimize lateral space and take advantage of the axial space. The platform is designed to be reconfigurable by varying link lengths of the parallel mechanisms and the baseline length between them. The specific requirements for the initial applications are as follows.

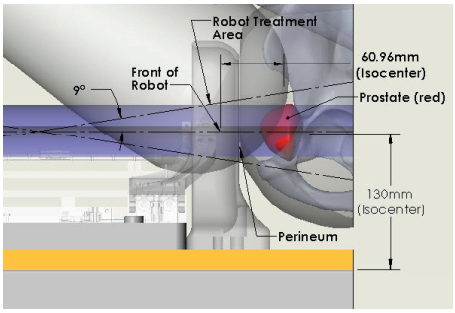

Fig. 2. A sagittal slice of the prostate (red) illustrates the necessity of needle angulation to facilitate pubic arch interference avoidance.

A. Design Requirement for Prostate Interventions

The average size of the prostate is $50mm$ in the lateral direction by $35mm$ in the anterior-posterior direction by $40mm$ in length. As shown in Fig. 2, needle angulation in the sagittal and coronal planes will enable procedure to be performed even when the needle pathway is contraindicated due to PAI [17]. The dimensions in this figure are based on five clinical patient trials and thus approximative because of the patient variability. To cover all volume of prostate and accommodate patient variability and lateral asymmetries in patient setup, the prostate is assumed to have the shape of a sphere with $50mm$ diameter. Thus, the required motion range of the robot is specified as follows: vertical motion is $100-150mm$, lateral motion is $\pm 25mm$, both pitch and yaw motion are $\pm 9°$.

B. Design Requirement for Neurosurgery

Since the 2-DOF alignment control is accomplished by a RCM mechanism, the manipulator is primarily used to provide Cartesian space positioning. Since the skull inside the scanner takes up about $25cm$, the width of the robot is limited to $20cm$. The axial motion is 15cm and the lateral motion is $5cm$. Further detail about the requirements can be found in [18].

III. Mechanism Design and Kinematic Analysis

Fig. 3 illustrates the structure of the 4-DOF surgical manipulator. Customized piezoelectric actuator driver with minimal image artifact is developed to control the piezoelectric actuators (PiezoMotor, Uppsala, Sweden). Standard rotary optical encoders (U.S. Digital, Vancouver, WA) are used for position sensing. MRI compatibility of the selected electromechanical systems [13], [19] indicates that the integrated system can utilize real-time MRI imaging to guide needle while scanning and a closed-loop image-guided surgery is possible. Global registration between the robot and image coordinates can be determined by MRI fiducials (MR Spots, Beekley, Bristol, CT) that are rigidly placed on the bottom plate of the robot.

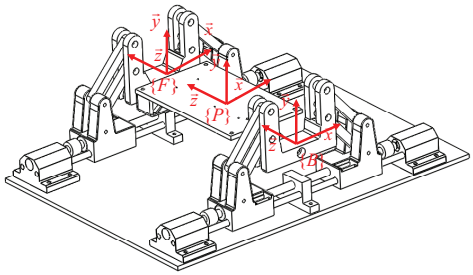

Fig. 3. Parallel surgical manipulator shown with defined coordinate systems of the rear stage (B) and the upper interface plate (P).

A. Mechanism Design

The robot consists of three major components: front stage, rear stage and the upper interface plate. Both the front stage and rear stage are 2-DOF motion module and share the same kinematic structure. In this design, the corresponding linkage lengths in the front stage and rear stage are the same. However, this link length is a design parameter than can be easily adjusted to achieve the required workspace. Each stage is composed of two four-bar mechanisms connected through a U-channel frame and each ground linkage of four-bar mechanism is driven by a cart that resides on a linear guide through plain bearings. Rotary piezoelectric motors located at the bottom housings are used to drive lead-screw mechanism to provide the prismatic motion of each carriage while all the revolute joints of the four-bar mechanism are passive.

To allow appropriate motion of the upper interface plate as the front and rear planar mechanisms are manipulated, the front U-channel frame is connected to the upper interface plate through one spherical joint. In the rear of upper interface plate, two rods are rigidly fixed with two revolute

joints respectively, and the rods are able to freely slide inside two rod-end bearings that are embedded inside the the back U-channel frame.

B. Kinematics and Workspace Analysis

The position and orientation of the upper interface plate is determined by the U-channel frame of the front and rear stage, and the center of the moving frames, as shown in Fig. 4, are denoted as $\overrightarrow{x}_F$ and $\overrightarrow{x}_B$. x_{1f} and x_{2f} are the position of the carts of front stage, while x_{1b} and x_{2b} are the position of the carts of back stage.

In Fig. 4, the center of front U-channel can be expressed as

$$\begin{cases} x_F = \frac{x_{1f}+x_{2f}}{2} \\ y_F = a - b + \sqrt{L_2^2 - (\frac{x_{2f}-x_{1f}-L_1}{2})^2} \end{cases} \tag{1}$$

where a is the distance between the x axis and bottom hole of the four-bar mechanism. b is the distance between the bottom hole and the baseline of the U-channel frame. L_1 is the U-channel frame width and L_2 is the length of the longer link (shown in blue) of the four-bar mechanism.

Similarly, the center of back U-channel can be expressed as

$$\begin{cases} x_B = \frac{x_{1b}+x_{2b}}{2} \\ y_B = a - b + \sqrt{L_2^2 - (\frac{x_{2b}-x_{1b}-L_1}{2})^2} \end{cases} \tag{2}$$

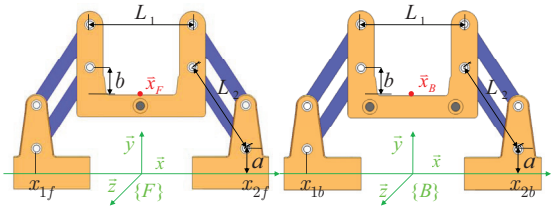

Fig. 4. Kinematics nomenclature of the front stage and rear stage.

With these positions, the center of the upper interface plate is expressed as

$$\begin{cases} x_P = \frac{x_F+x_B}{2} \\ y_P = \frac{y_F+y_B}{2} \end{cases} \tag{3}$$

While the pitch angle θ and yaw angle φ are expressed as

$$\theta = \text{atan2}(y_f - y_b, D) \tag{4}$$

$$\varphi = \text{atan2}(x_f - x_b, D) \tag{5}$$

where D is the distance between the front stage and rear stage.

Robot inverse kinematics can also be derived based on the above kinematic relationship. If the linkage parameters are determined as $a = 30mm$, $b = 20mm$, $L_1 = 96mm$ and $L_2 = 65mm$, the workspace of the planar mechanism (green dots) is overlaid with the prostate model (red circle) as shown in Fig. 5. The range of x_{1f}, x_{2f} and x_{1b}, x_{2b} have the same range of motion $[-20mm, 120mm]$ in this figure.

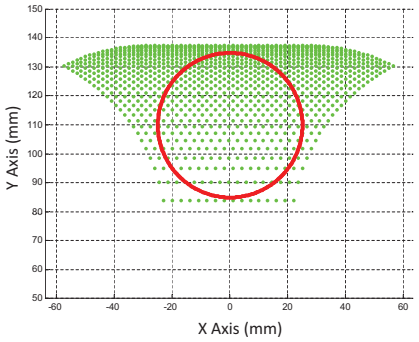

Fig. 5. Workspace of the planar mechanism (front and rear stage), represented as green dots, that covers the whole volume of a generic prostate approximated as sphere with $5cm$ diameter (red circle)

IV. System Integration and Preliminary Validation

A prototype of the surgical manipulator has been constructed as shown in Fig. 6. This section describes system integration and preliminary validation.

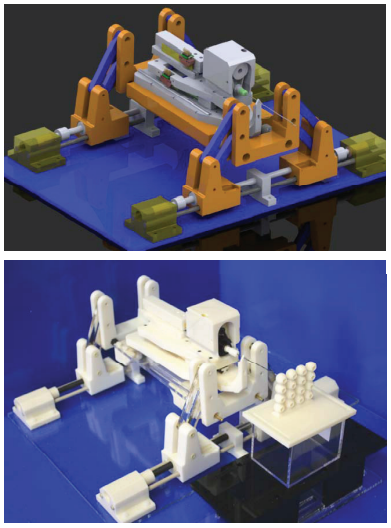

Fig. 6. The 4-DOF manipulator is integrated with a 3-DOF needle driver module is to provide 7-DOF needle motion for prostate interventions.

A. Integration with Needle Driver for Prostate Interventions

As a base platform for prostate interventions, the 4-DOF base manipulator is integrated with a 3-DOF needle driver that provides needle translation, rotation and stylet retraction to provide 7-DOF needle motion. The needle guide of the needle driver is able to accommodate standard medical needles with different diameters and the driver module is described in [9]. In general, the scalability, size and robustness of electromechanical systems in this system present a clear advantage over our prior pneumatically actuated system [16], in particular for small range needle motion and dynamic performance.

B. Integration with Remote Center Motion Mechanism for Neurosurgery

By virtue of the reconfigurable feature of the surgical manipulator, the same mechanism is easily adapted to a

platform for our neurosurgery manipulator. Two connecting rods are placed on top of the front and back carts to mechanically synchronize the motion of front and back stages, while to reduce the 4-DOF manipulator to 2-DOF structure. Timing belts and timing pulley are used to transmit the motion of the rotary motor from back carts to front carts. A linear rail actuated by a lead-screw mechanism is used to provide a translational motion DOF along the axis of bore and this makes this system have 3-DOF Cartesian positioning capability. The RCM cannula guide is placed on top of the manipulator as shown in Fig. 7.

Fig. 7. The reconfigured manipulator is integrated with a 2-DOF remote center of motion mechanism to provide 5-DOF control of a cannula guide for stereotactic neurosurgery.

V. Discussion

In this paper, we presented a modular design approach for robotic surgical manipulator under MRI guidance. This modular manipulator integrated with different end-effector modules is investigated for prostate brachytherapy and neurosurgery applications. Future work includes robot motion control experiments, integration of fiducial-based tracking frames and accuracy evaluation. The intent of the device is to serve as slave robot with fiber optic force sensing [20], [21] to perform teleoperated needle placement with inside MRI scanner [9], [22].

VI. Acknowledgements

This work is supported by the Congressionally Directed Medical Research Programs Prostate Cancer Research Program (CDMRP PCRP) New Investigator Award W81XWH-09-1-0191. Thanks to Dr. Everette Burdette and Dr. Junichi Tokuda for the prostate CAD model.

References

[1] M. G. Schouten, J. Bomers, D. Yakar, H. Huisman, D. Bosboom, T. W. J. Scheenen, S. Misra, and J. J. Futterer, "Evaluation of a robotic technique for transrectal MRI-guided prostate biopsies," in *International Society for Magnetic Resonance in Medicine*, 2011.

[2] E. Yeniaras, J. Lamaury, N. Navkar, D. Shah, K.Chin, and N. Tsekos, "Virtual Reality Enhanced Control of A Robotic Manipulator for Image Guided Interventions in the Beating Heart," in *IEEE International Conference on Robotics and Automation*, 2011.

[3] H. Elhawary, A. Zivanovic, M. Rea, B. Davies, C. Besant, I. Young, and M. Lamperth, "A modular approach to MRI-compatible robotics," *Engineering in Medicine and Biology Magazine, IEEE*, vol. 27, no. 3, pp. 35–41, 2008.

[4] M. Muntener, A. Patriciu, D. Petrisor, D. Ursu, D. Y. Song, and D. Stoianovici, "Transperineal prostate intervention: robot for fully automated mr imaging–system description and proof of principle in a canine model.," *Radiology*, vol. 247, pp. 543–549, May 2008.

[5] N. Miyata, E. Kobayashi, T. Dohi, H. Iseki, and K. Takakura, "Micro-grasping forceps manipulator for mr-guided neurosurgery," in *Medical Image Computing and Computer-Assisted Intervention*, vol. 2488 of *LNCS*, pp. 107–113, 2002.

[6] Y. Koseki, T. Tanikawa, and K. Chinzei, "MRI-compatible micromanipulator; design and implementation and MRI-compatibility tests," in *Annual Conference of IEEE Engineering in Medicine and Biology Society*, pp. 465–468, 2007.

[7] H. Su, M. Zervas, G. Cole, C. Furlong, and G. Fischer, "Real-time MRI-Guided Needle Placement Robot with Integrated Fiber Optic Force Sensing," in *IEEE ICRA 2011 International Conference on Robotics and Automation*, (Shanghai, China), 2011.

[8] S. Abdelaziz, L. Esteveny, P. Renaud, B. Bayle, L. Barbe, M. De Mathelin, and A. Gangi, "Design considerations for a novel MRI compatible manipulator for prostate cryoablation," *International Journal of Computer Assisted Radiology and Surgery*, pp. 1–9, 2011.

[9] H. Su, G. Cole, and G. S. Fischer, "High-field MRI-Compatible needle placement robots for prostate interventions: pneumatic and piezoelectric approaches," in *Advances in Robotics and Virtual Reality* (T. Gulrez and A. Hassanien, eds.), Springer-Verlag, 2011.

[10] H. Su, W. Shang, G. Cole, K. Harrington, and F. S. Gregory, "Haptic system design for MRI-guided needle based prostate brachytherapy," IEEE Haptics Symposium 2010, (Boston, MA, USA), IEEE, 2010.

[11] H. Su, G. Cole, N. Hata, C. Tempany, and G. Fischer, "Real-time MRI-Guided Transperineal Needle Placement Prostate Interventions with Piezoelectrically Actuated Robotic Assistance," in *Radiological Society of North America 97th Scientific Assembly and Annual Meeting*, (Chicago, USA), December 2011.

[12] H. Su, A. Camilo, G. Cole, N. Hata, C. Tempany, and G. Fischer, "High-field MRI compatible needle placement robot for prostate interventions," in *Proceedings of MMVR18 (Medicine Meets Virtual Reality)*, (Newport Beach, California, USA), February 2011.

[13] G. Cole, K. Harrington, H. Su, A. Camilo, J. Pilitsis, and G. Fischer, "Closed-Loop Actuated Surgical System Utilizing Real-Time In-Situ MRI Guidance," in *12th International Symposium on Experimental Robotics - ISER 2010*, (New Delhi and Agra, India), Dec 2010.

[14] E. Yeniaras, J. Lamaury, Y. Hedayati, N. V. Sternberg, and N. V. Tsekos, "Prototype cyber-physical system for magnetic resonance based, robot assisted minimally invasive intracardiac surgeries," *International Journal of Computer Assisted Radiology and Surgery*, 2011.

[15] B. Yang, U. Tan, R. Gullapalli, A. McMillan, and J. Desai, "Design and Implementation of a Pneumatically-Actuated Robot for Breast Biopsy under Continuous MRI," in *IEEE ICRA 2011 International Conference on Robotics and Automation*, (Shanghai, China), 2011.

[16] S. E. Song, N. B. Cho, G. Fischer, N. Hata, C. Tempany, G. Fichtinger, and I. Iordachita, "Development of a Pneumatic Robot for MRI-Guided Transperineal Prostate Biopsy and Brachytherapy: New Approaches," in *IEEE Int Conf on Robotics and Automation*, 2010.

[17] G. S. Fischer, I. I. Iordachita, C. Csoma, J. Tokuda, S. P. DiMaio, C. M. Tempany, N. Hata, and G. Fichtinger, "MRI-Compatible Pneumatic Robot for Transperineal Prostate Needle Placement," *IEEE/ASME Transactions on Mechatronics*, vol. 13, June 2008.

[18] G. A. Cole, J. G. Pilitsis, and G. S. Fischer, "Design of a Robotic System for MRI-Guided Deep Brain Stimulation Electrode Placement," in *IEEE Int Conf on Robotics and Automation*, May 2009.

[19] G. Fischer, G. Cole, and H. Su, "Approaches to creating and controlling motion in MRI (invited paper)," in *Proc. Annual Int Engineering in Medicine and Biology Society (EMBC) Conf. of the IEEE*, 2011.

[20] H. Su, M. Zervas, C. Furlong, and G. S. Fischer, "A miniature MRI-compatible fiber-optic force sensor utilizing Fabry-Perot interferometer," MEMS and Nanotechnology, Conference Proceedings of the Society for Experimental Mechanics Series, pp. 131–136, 2011.

[21] H. Su and G. Fischer, "A 3-axis optical force/torque sensor for prostate needle placement in magnetic resonance imaging environments," 2nd Annual IEEE International Conference on Technologies for Practical Robot Applications, (Boston, MA, USA), pp. 5–9, IEEE, 2009.

[22] S. E. Song, R. Seifabadi, A. Krieger, J. Tokuda, G. Fichtinger, and I. Iordachita, "Robotic System for MRI-guided Prostate Intervention: Feasibility Study of Tele-operated Needle Insertion," *Computer Aided Radiology and Surgery*, 2011.